Development 138, 1459-1469 (2011) doi:10.1242/dev.058156

Clonal analysis by distinct viral vectors identifies bona fide neural stem cells in the adult zebrafish telencephalon and characterizes their division properties and fate

Ina Rothenaigner[1,2,*], Monika Krecsmarik[1,*], John A. Hayes[3], Brigitte Bahn[2,†], Alexandra Lepier[4], Gilles Fortin[3], Magdalena Götz[4,5], Ravi Jagasia[6] and Laure Bally-Cuif[1,2,‡]

SUMMARY

Neurogenesis is widespread in the zebrafish adult brain through the maintenance of active germinal niches. To characterize which progenitor properties correlate with this extensive neurogenic potential, we set up a method that allows progenitor cell transduction and tracing in the adult zebrafish brain using GFP-encoding retro- and lentiviruses. The telencephalic germinal zone of the zebrafish comprises quiescent radial glial progenitors and actively dividing neuroblasts. Making use of the power of clonal viral vector-based analysis, we demonstrate that these progenitors follow different division modes and fates: neuroblasts primarily undergo a limited amplification phase followed by symmetric neurogenic divisions; by contrast, radial glia are capable at the single cell level of both self-renewing and generating different cell types, and hence exhibit bona fide neural stem cell (NSC) properties in vivo. We also show that radial glial cells predominantly undergo symmetric gliogenic divisions, which amplify this NSC pool and may account for its long-lasting maintenance. We further demonstrate that blocking Notch signaling results in a significant increase in proliferating cells and in the numbers of clones, but does not affect clone composition, demonstrating that Notch primarily controls proliferation rather than cell fate. Finally, through long-term tracing, we illustrate the functional integration of newborn neurons in forebrain adult circuitries. These results characterize fundamental aspects of adult progenitor cells and neurogenesis, and open the way to using virus-based technologies for stable genetic manipulations and clonal analyses in the zebrafish adult brain.

KEY WORDS: Retroviral transduction, Adult neurogenesis, Neural stem cells, Notch

INTRODUCTION

Adult neurogenesis is one of the most remarkable forms of structural plasticity in the brain of vertebrates, including human. To date, our knowledge of this process mostly comes from studying the rodent brain. There, adult neurogenesis is constitutive from two restricted telencephalic areas, the subependymal zone (SEZ) of the lateral ventricle and the subgranular zone (SGZ) of the hippocampus (Lledo et al., 2006; Zhao et al., 2008). In these domains, glial cells with characteristics of neural stem cells (NSCs) are involved in generating neurons that integrate into the olfactory bulb (OB) and hippocampal circuitries (Kriegstein and Alvarez-Buylla, 2009). Although the precise physiological role of adult neurogenesis remains elusive, understanding its molecular and cellular bases is of crucial therapeutical interest. Recently, for example, proof of principle was obtained that boosting neuronal production in pathological aging could delay cognitive decline (Deng et al., 2010; Pieper et al., 2010).

The zebrafish, *Danio rerio*, has emerged as a powerful model to study adult neurogenesis. Contrary to mammals, domains of constitutive proliferation and neurogenesis are found in all brain subdivisions of the adult zebrafish, and these domains can generate a variety of neuronal subtypes (Adolf et al., 2006; Grandel et al., 2006; Pellegrini et al., 2007; Zupanc et al., 2005). Therefore, the zebrafish is an excellent comparative model to address issues of neuro-regenerative biology, including which mechanisms can sustain widespread adult NSC activation and fate choices.

The zebrafish telencephalic ventricular zone (VZ) hosts a large majority (~90%) of radial glia (Chapouton et al., 2010; Ganz et al., 2010; März et al., 2010). Proliferation markers such as PCNA (proliferating cell nuclear antigen) allowed the identification of three VZ cell types: PCNA-negative radial glia (‘type I’ cells), PCNA-positive radial glia (‘type II’) and dividing non-glial progenitors (‘type III’). Type III cells express markers of committed precursors (*ascl1a*, PSA-NCAM) and are probably neuroblasts (Chapouton et al., 2010; März et al., 2010). Manipulations of Notch activity further suggest that type I and II cells represent two states of the same quiescent and/or slow-dividing progenitor population, which are probably the NSCs in this brain area (Chapouton et al., 2010). These different cell types could be found through the entire dorsoventral extent of the VZ,

[1]Zebrafish Neurogenetics Group, Laboratory of Neurobiology and Development (N&D), CNRS UPR 3294, Institute of Neurobiology Alfred Fessard, Avenue de la Terrasse, 91198 Gif-sur-Yvette cédex, France. [2]Department Zebrafish Neurogenetics, Helmholtz Center Munich, German Research Center for Environmental Health, Ingolstaedter Landstrasse 1, 85764 Neuherberg, Germany. [3]Hindbrain Integrative Neurobiology, Laboratory of Neurobiology and Development (N&D), CNRS UPR 3294, Institute of Neurobiology Alfred Fessard, Avenue de la Terrasse, 91198 Gif-sur-Yvette cédex, France. [4]Department of Physiological Genomics, Institute of Physiology, Ludwig-Maximilians University Munich, Schillerstrasse 46, 80336 Munich, Germany. [5]Institute for Stem Cell Research, Helmholtz Center Munich, German Research Center for Environmental Health, Ingolstaedter Landstrasse 1, 85764 Neuherberg, Germany. [6]F. Hoffmann-La Roche, CNS Discovery Research, Building 069 R. 239A, 4070 Basel, Switzerland.

*These authors contributed equally to this work
†Present address: Roche Diagnostics GmbH, Nonnenwald 2, 82377 Penzberg, Germany
‡Author for correspondence (bally-cuif@inaf.cnrs-gif.fr)

Accepted 24 January 2011

encompassing (but also extending largely beyond) the domains that are potentially homologous to the mammalian SEZ and SGZ (März et al., 2010). Thus, a better characterization of this system may help provide a more comprehensive understanding of the existing repertoire of NSCs and neurogenesis modes. To date, the endogenous fate of type I cells could not be assessed for lack of a means to label this non-dividing cell state. A related question is which of the different progenitor types exhibit distinctive NSC properties, i.e. self-renewal and multipotentiality. Third, the cell division modes of type I/II cells, and in particular how they replenish/maintain their pool, was not determined. In addition, whether and when adult-born neurons become integrated in the telencephalic circuitry is not known.

Several of these aspects in the rodent adult brain have been delineated based on retroviral GFP (green fluorescent protein) transduction (Carleton et al., 2003; Ge et al., 2006; Nissant et al., 2009; Suh et al., 2007; Toni et al., 2008; Toni et al., 2007; Zhao et al., 2006). Here, having established this technique for progenitors of the zebrafish adult brain, we further characterized cell lineage, cell fate and neuronal maturation in this system.

MATERIALS AND METHODS

Fish strains

Three- to nine-month-old *Danio rerio* of both sexes from the wild-type strains AB and EK were used.

(Virus-)plasmids

The MLV-based retroviral vectors used (see Fig. S1A in the supplementary material) express GFP under the *EF1α* (Elongation factor *1α*) (Ge et al., 2006) or the *CAG* (cytomegalovirus immediate early enhancer-chicken β-actin) promoter (Zhao et al., 2006). The lentiviral vectors used (see Fig. S1B in the supplementary material) carry the *CMV* (cytomegalovirus) (Pfeifer et al., 2001) or the *EF1α* promoter (pWPI, http://tronolab.epfl.ch/). All viral vectors used are self-inactivating. *pCS2:GFP* (Muller et al., 2000) was used as a transfection control.

Virus production

Replication-incompetent GFP-expressing murine retroviruses were produced from a packaging cell line (GPG-293) (Ory et al., 1996) transiently transfected with the retroviral expression plasmid. Lentiviral vectors were produced by transient co-transfection of HEK 293T cells with lentiviral packaging plasmid pCMVDR8.9, pseudotyping plasmid pVSVG (http://tronolab.epfl.ch) and the lentiviral expression plasmid. The supernatant was harvested 48 and 72 hours after transfection, centrifuged and filtered through a 0.45 μm filter (Millipore). Viral particles were pelleted at 50,000 ***g*** at 4°C for 2 hours, resuspended in TBS-5 [50 mM Tris-HCl (pH 7.8), 130 mM NaCl, 10 mM KCl, 5 mM $MgCl_2$] and stored at –80°C. Viral titers ranged between 10^7 and 10^9 infectious particles per ml (on 293T cells).

In vivo injections

Fish preparation was performed as described previously (Chapouton et al., 2010). The viral resuspension (≤ 0.5 μl), supplemented with Fast Green dye (Sigma), was pressure injected into the brain ventricle with a glass capillary. Afterwards, the fish was placed for 20 minutes in fresh water containing penicillin-streptomycin (pen-strep) (100 U/ml) then kept for 24 hours at 37°C. Control injections used FluoSpheres [Invitrogen, carboxylate-modified microspheres, 0.04 μm, yellow-green fluorescent (505/515)] diluted 1:10 in 110 mM NaCl.

Cell culture and flow cytometry analysis

Human HEK 293T cells were cultured in DMEM, 10% fetal calf serum (FCS), 1% pen-strep in an H_2O-saturated atmosphere with 5% CO_2 at 37°C. Zebrafish PAC2 fibroblasts (He et al., 2006; Lin et al., 1994) were cultured in Leiboltz medium containing 20% FCS, 1% pen-strep at 28°C. Cells were seeded at 1.5×10^5 cells per well in 24-well plates 1 day prior to infection or transfection. Transfections used Lipofectamine (Invitrogen) according to the manufacturer's protocol. Infections were performed by replacing the culture medium with fresh medium containing virus solution. Cells were harvested and FACS analyzed for their expression of GFP 3 days after transfection and 4 days after infection using a FACScalibur flow cytometer (Becton Dickinson). To gate the fluorescent cell population, non-transduced cells were analyzed.

Analysis of cell divisions upon Notch blockade

We compared the γ-secretase inhibitor DAPT (Chapouton et al., 2010) with a dose range of its second-generation derivative, LY411575 (Fauq et al., 2007). LY411575 (10 μM) proved as efficient as 100 μM DAPT in interfering with Notch signaling (not shown). Adult fish were injected with Lenti-*CMV:GFP* three times at 7-day intervals. After a 2-week chase, they were treated for 48 hours with 10 μM LY411575 in the swimming water at 28°C (see Fig. 6F). Virus-injected control fish were treated with the same final concentration (0.04%) of DMSO carrier. Eight brains (80 sections) were analyzed for each treatment.

Chlorodeoxyuridine incorporation

Zebrafish were kept in tank water containing 0.2 mM of the thymidine analogue 5-chloro-2′-deoxyuridine CldU (Sigma C6891) at 28°C for 24 hours, followed by a chase period in fresh tank water.

Immunohistochemistry

Immunohistochemistry was performed as described previously (Chapouton et al., 2010). The following primary antibodies were used: S100β (rabbit, 1:2000, Dako), GFP (chicken, 1:1000, Aves Laboratories), PCNA (mouse, 1:250, Dako), HuC/D (mouse, 1:600, Invitrogen or human, 1:2000, a gift from Dr B. Zalc, Salpêtrière Hospital, Paris, France), cleaved caspase 3 (rabbit, 1:500, Cell Signaling), BrdU (rat, 1:250, Abcam) and SV2 (mouse, 1:200, Developmental Studies Hybridoma Bank). Secondary antibodies were raised in goat and coupled to AlexaFluor dyes (488, 555 or 647; 1:1000, Invitrogen).

Imaging and cell counting

Immunostainings were documented on a Zeiss LSM510Meta or on a Zeiss LSM700 confocal microscope using the 20×/40× water-immersion and the 63×/100× oil-immersion objectives, and were processed using the LSM software. Composite images, such as Fig. 4A,B, were automatically stitched upon acquisition using 'Tilescan' mode on the Zeiss ZEN software. For virus-infected cells, counting was carried out manually using the LSM Image Examiner software on single optical sections ($n\geq4$ infected brains per virus type). For the quantification of CldU-, cleaved caspase-3- and HuC/D-positive cells, 50 μm serial sections through the whole telencephalon were prepared ($n=4$ brains for each time point analyzed). Counting was carried out manually on *z*-stacks taken with a 20× objective in each section. Statistical significance was assessed using Fisher's or *t*-test.

Electrophysiology

Carbogen-bubbled (95% O_2/5% CO_2) artificial cerebrospinal fluid (ACSF) was used for dissections and recordings, and contained (in mM): 104 NaCl, 6.9 KCl, 0.5 NaH_2PO_4, 18.2 $NaHCO_3$, 26 D-glucose, 1.1 $CaCl_2$ and 0.87 $MgCl_2$, and was calibrated to pH 7.4 with NaOH or HCl. Brains were removed and embedded in 4% agar. Slices for in vitro electrophysiological recordings (350 μm) were cut in the horizontal plane on a Leica VT1000S microtome. They were placed into a chamber containing continuously perfused ACSF. Positioning of patch pipettes onto GFP-positive cells was carried out using a standard epifluorescence microscope (Eclipse-FN1 upright microscope; Nikon, Tokyo, Japan) equipped with FITC and Cy3 filter cubes. An X-Cite 120Q lamp (Lumen Dynamics Group, Mississauga, Ontario, Canada) was used for epifluorescence excitation. Visually controlled patch recordings were then performed on the identified cells using differential interference contrast microscopy and infrared illumination (IR-DIC) at room temperature using an Axon Multiclamp 700B patch-clamp amplifier and a Digidata 1440A analog-to-digital (DAC) converter using pClamp 10 and Multiclamp Commander software from Molecular Devices (Sunnyvale, CA, USA). Patch pipettes (5-10 MΩ bath resistance) were pulled from borosilicate glass (GC 150TF; Clark

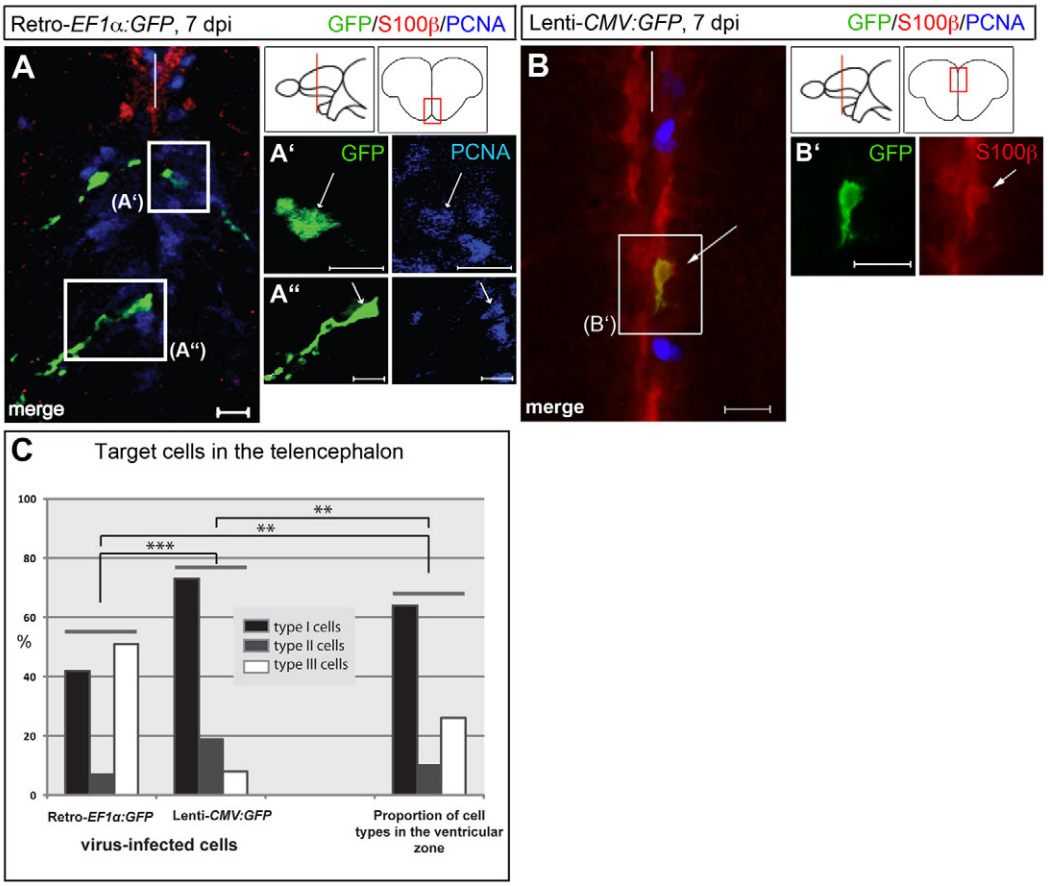

Fig. 1. Retro- and lentiviruses differently target the telencephalic ventricular cell types. (**A**,**B**) Typical examples of the main cell type targeted by Retro-*EF1α:GFP* (A) and Lenti-*CMV:GFP* (B) infections at 7 dpi. Immunostaining for GFP (green), radial glia (S100β, red) and the proliferation marker PCNA (blue) is shown in the telencephalon (80 μm coronal sections; single optical planes observed by confocal microscopy; dorsal upwards; section plane and position of the micrographs shown on the cartoons; ventricle indicated by white bars). (**A′**,**A″**,**B′**) Higher magnifications of the single channels. Scale bars: 10 μm. Arrows indicate the transduced cells of interest. (**C**) Quantification at 7 dpi of the proportion of cell types I, II and III transduced with the two viruses (left bars, counted across the whole telencephalic VZ). Retroviral infection: 42% type I, 7% type II, 51% type III cells (60 cells from four brains). Lentiviral infection: 73% type I, 19% type II, 8% type III cells (26 cells from four brains). The right panel shows the normal distribution of the three cell types in the telencephalic VZ (type I, 64%; type II, 10%; type III, 26%) (3006 cells counted). Fisher's test: ***P*=0.001314 and *P*=0.001330 (comparison of the proportion of retrovirus-transduced cells and lentivirus-transduced cells, respectively, with the uninfected situation); ****P*=0.0001295.

Electromedical Instruments, Pangbourn, UK) and were filled with the following solution (in mM): 116 potassium gluconate, 19.8 KCl, 0.5 EGTA, 9.4 HEPES, 2.8 $MgCl_2$, 0.06 mg/ml Alexa 594. Cell-attached patch recordings were performed with high seal resistances ($R_s \gg 1$ GΩ) to probe for spontaneous discharges of action potentials. Fluorescence images and IR-DIC images were acquired with MetaVue 7.5 software (Universal Imaging Corporation, West Chester, PA, USA) and a cooled CCD camera (CoolSnap HQ2; Photometrics, Tucson, AZ, USA). Fluorescence images were processed using ImageJ (NIH, Bethesda, MD, USA).

RESULTS

Retro- and lentiviruses efficiently transduce ventricular cells of the zebrafish adult brain

We assayed different retroviral and lentiviral constructs (see Fig. S1A,B in the supplementary material) for their efficiency to drive GFP expression after DNA transfection (see Fig. S1C,D, upper panels, in the supplementary material) and viral infection (see Fig. S1C,D, lower panels, in the supplementary material) of zebrafish cells. All viruses tested were pseudotyped by the glycoprotein of the vesicular stomatitis virus (VSV-G), which is very stable, allows production of viruses with high titers and permits gene delivery in an extensive range of cell types from different species, including zebrafish (Burns et al., 1993; Chen et al., 2002; Lin et al., 1994).

Using retroviruses in zebrafish Pac2 fibroblasts, we could only detect expression driven by *EF1α*. Surprisingly, the *CAG* (*CMV early enhancer/chicken β actin*) promoter, which avoids promoter silencing and is widely used in rodents to study adult neurogenesis (Brill et al., 2008; Zhao et al., 2006), was inefficient (see Fig. S1C in the supplementary material). Both lentiviral constructs, whether using *CMV* or *EF1α*, showed expression after transfection. After infection, however, only the *CMV*-driven construct mediated GFP expression (see Fig. S1D in the supplementary material).

Next, we assayed the capacity of retro- and lentiviruses to target zebrafish adult neural progenitor cells (NPCs) in vivo. Many proliferation zones in the zebrafish adult brain being situated at or near the ventricular surface, we injected the viral suspensions into the brain ventricle (see Fig. S1E,F in the supplementary material) (>5000 viral particles per brain) and GFP expression was monitored after 7 days. This delay was necessary to accumulate

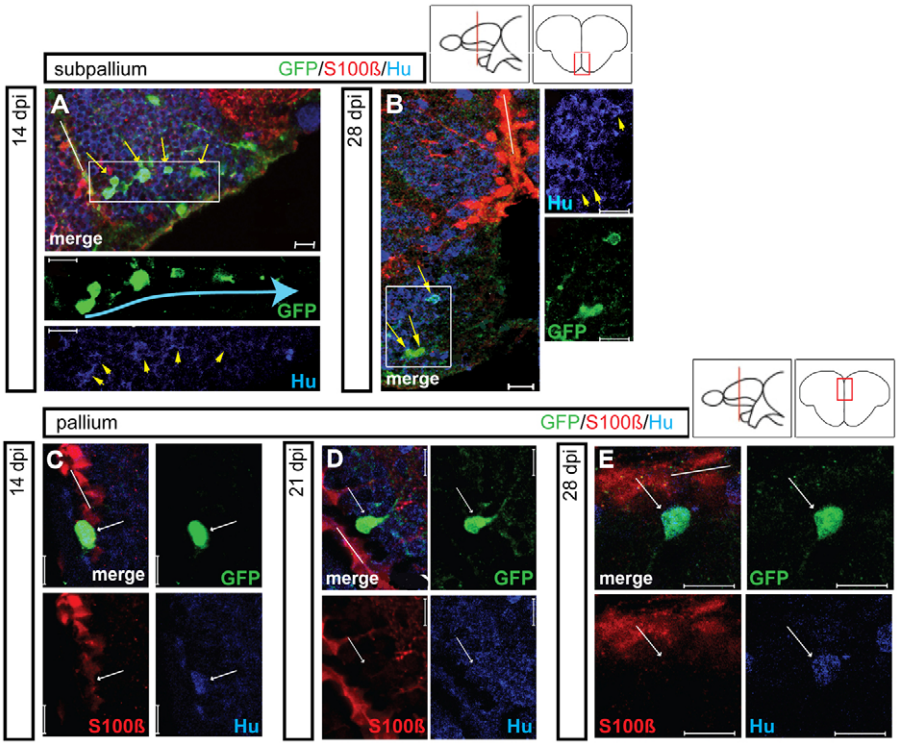

Fig. 2. Maturation of GFP-positive cells into newborn neurons in the subpallial and pallial regions. Maturation was followed in the subpallium (upper panels) and pallium (lower panels) at various time points after infection (14, 21 and 28 dpi) (single optical sections from Retro-*EF1α:GFP*-injected brains, immunostained for GFP, S100β and/or HuC/D, white bars indicate the VZ). (**A**,**B**) In the subpallium, the majority of GFP-positive cells express HuC/D at 14 dpi (A, yellow arrows). Some labeled cells seem to move away from the VZ in chain-like assemblies (blue arrow). At 28 dpi, newborn neurons (yellow arrows) are small and exhibit short processes. Single-channel views are magnifications of the boxed areas. In B, all three cells indicated are HuC/D positive. (**C-E**) In the pallium, newborn HuC/D-positive neurons (white arrows) are still located close to the VZ at 28 dpi. Scale bars: 10 μm.

GFP levels detectable by immunocytochemistry. We recovered GFP-expressing cells with both virus types, distributed along the whole VZ (see Fig. S1G-L in the supplementary material), even 3 months after infection (see Fig. 3B).

Retro- and lentiviruses target the different VZ progenitor subtypes in different proportions

We next characterized the cell types targeted by the two viruses, focusing on the telencephalon, where ventricular NPCs have been best characterized (Chapouton et al., 2010; Ganz et al., 2010; März et al., 2010). In the mammalian context, these virus types target differently the diverse NPCs (Colak et al., 2008): the reverse-transcribed genetic material of simple retroviruses such as MLV only integrates into dividing cells; by contrast, more complex retroviruses such as lentiviruses can integrate into non-dividing cells.

We stained infected brains with the radial glia marker S100β and the proliferation marker PCNA to quantify at 7 days post-infection (dpi) the proportion of state I, II and III cells transduced in the whole telencephalon. Typically, following lentiviral infection, GFP-transduced cells were predominately type I cells (S100β-positive, PCNA-negative) (Fig. 1B,C) (73%, *n*=26 cells counted). By contrast, with retroviruses, the predominant GFP-positive cell type among populations I-III was type III (PCNA-positive, GFAP-negative cells) (Fig. 1A,C) (51%, *n*=60 cells counted). The presence of GFP-transduced type I cells in the latter case is in agreement with previous BrdU tracings showing that PCNA-negative radial glia are generated at the adult VZ from dividing progenitors (Chapouton et al., 2010). The differences in cell type distribution between the two viruses are statistically significant (Fig. 1C), and also significantly differ from the normal distribution of cell types along the VZ in uninfected brains (Fig. 1C, histogram to the right). Hence, using lentiviruses will bias towards tracing type I cells, and retroviruses towards type III. In addition, retrovirus-transduced cells expressing neither S100β nor PCNA could be found in a high proportion (53% of GFP-positive cells), probably representing immature neurons (not shown).

Newborn neurons populating the telencephalon mature over 4-8 weeks and functionally integrate into local circuitries

We next conducted long-term experiments to characterize the fate of adult-born neurons. Retroviruses were used in this analysis to favor tracing active progenitors and enrich transduced brains in GFP-positive neurons. In agreement with previous reports (Adolf et al., 2006), a significant proportion (39%, *n*=11 brains) of GFP-positive cells expressing HuC/D was observed in the subpallium already 1 week after infection (not shown). At 14 dpi, a large majority of the GFP-positive cells were located outside the VZ and stained positive for HuC/D (83%, *n*=9 brains) (Fig. 2A). Morphological characterization revealed that these neurons, at 28 dpi (Fig. 2B) and later (not shown), did not develop long axons and were of small size (~5 μm in diameter). Pallial regions mostly revealed single HuC/D-positive cells (Fig. 2C-E). These newborn neurons migrated very slowly and were still present within less than a few cell diameters from the VZ after 28 days (Fig. 2E). Compared with subpallial neurons, they exhibited larger cell bodies and long, often multipolar, processes (see Fig. 5E).

To determine whether and when adult-born neurons receive synaptic input, we carried out immunohistochemical detection of the synaptic vesicle protein SV2 (Jontes et al., 2004; Niell et al., 2004) on retrovirus-transduced brains. In the OB internal layer, which hosts a large proportion of the newborn neurons originating from the subpallial VZ (Adolf et al., 2006; Grandel et al., 2006), we detected GFP-positive cells surrounded by SV2 contacts at 28 dpi (Fig. 3A). Within the same time frame, and at least until 84 dpi (12 weeks), SV2-positive GFP-positive neurons were observed in the subpallium proper (Fig. 3B). In the pallium, neuronal processes

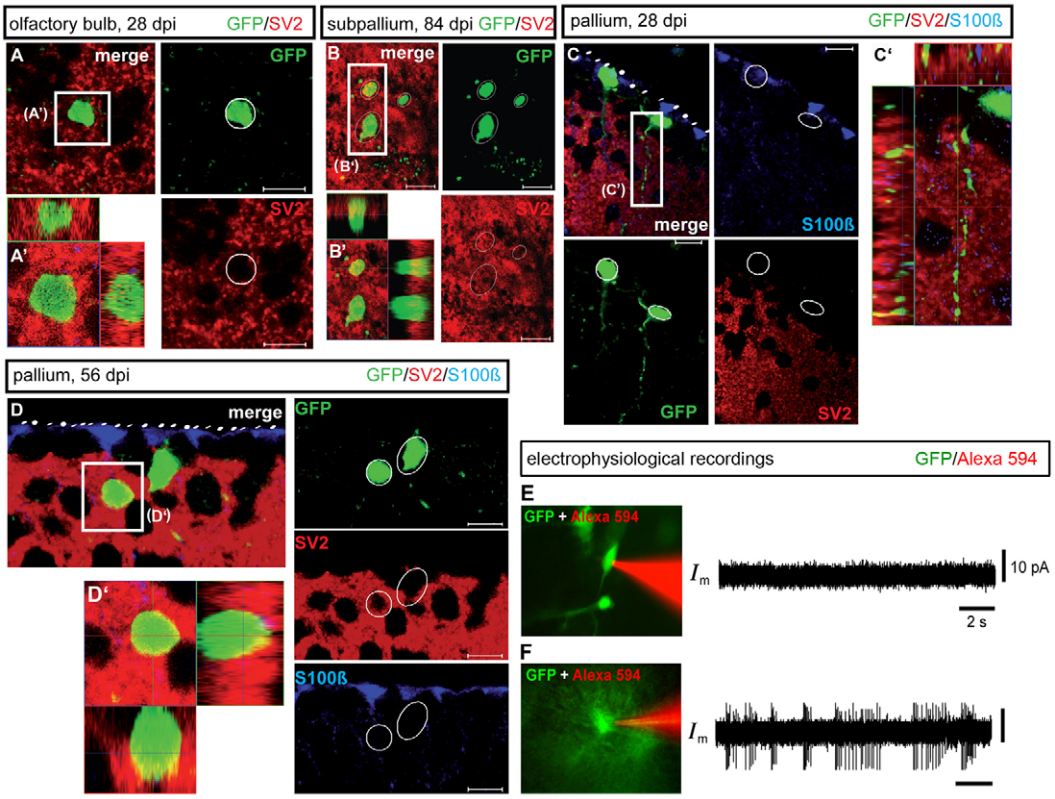

Fig. 3. Structural and functional integration of adult-born neuron into existing forebrain neuronal networks. (**A-D′**) Immunohistochemical detection of GFP (green), S100β (blue) and the synaptic marker SV2 (red) on cross-sections of the OB (A,A′), subpallium (B,B′) or pallium (C-D′) at 28, 56 or 84 dpi (confocal *z*-section images and orthogonal projections). Scale bars: 10 μm. (**E**,**F**) Cell-attached electrophysiological recordings of GFP-positive cells. (E) Example of a GFP-positive cell 2 weeks post-infection that did not exhibit spontaneous action potentials. (F) Example of a GFP-positive cell 7 weeks post-infection with spontaneous action potentials (green, GFP-positive cells; red, contents of the patch pipette). Both right-panel horizontal and vertical scale bars are the same in E and F.

were covered with SV2 contacts at 28 dpi (Fig. 3C), and labeling of neuronal soma was observed at 56 dpi (Fig. 3D). These results suggest that newborn neurons become functionally integrated into the existing forebrain circuitries within 4-8 weeks after their generation. To reinforce this conclusion, we sought to verify that GFP-positive cells display characteristics of functional neurons by conducting electrophysiological recordings during the neuronal maturation phase. Acute horizontal brain slices were prepared at 7-day intervals between 2 and 8 weeks post-infection (wpi), and six GFP-positive cells were patched in cell-attached configuration. This recording configuration is advantageous for reflecting the endogenous activity of targeted cells because it avoids intracellular dialysis that is expected to occur in whole-cell patch recordings, which could be particularly problematic for small cells. Two out of six cells, aged 7 and 8 wpi, featured spontaneous discharges of action potentials (Fig. 3F; and not shown) and can be considered as bona fide neurons, while the remaining cells (aged 2 to 4 wpi) displayed no evidence of spontaneous spikes, precluding the determination of their neuronal or glial nature (Fig. 3E; not shown). These data further support the view that, during neuronal maturation, GFP-positive cells may become integrated into existing circuitries.

It was reported in mouse that the integration phase of adult-born neurons coincides with a massive period of cell death (Lledo and Saghatelyan, 2005; Petreanu and Alvarez-Buylla, 2002; Winner et al., 2002). We evaluated this issue in zebrafish by focusing on the pallium, where newborn neurons do not exhibit extensive migration. We observed a loss of GFP-positive neurons after 21 dpi (see Fig. S2A in the supplementary material). To assess for cell death events, we labeled type III cells by a brief pulse of the thymidine analogue CldU and monitored expression of the apoptotic marker Caspase 3 (Jackson-Lewis et al., 2000; Jeon et al., 1999) in cells double-positive for CldU and HuC/D after 14, 21 or 56 days of chase. The proportion of dying neurons within the newborn population was overall very low (below 1.5% at each time point), and did not significantly vary during the period analyzed (see Fig. S2B,C in the supplementary material). Hence, unlike in mouse, we failed to detect extensive neuronal death during the maturation period. Promoter silencing may already occur in newborn neurons during this phase and might mostly account for the observed loss of GFP-positive neurons.

Type I and III progenitors follow different division modalities

We next took advantage of viral transduction in clonal analyses to determine which cell division modes occur at the telencephalic VZ. We analyzed brains with, at most, five transduced cell clones per cerebral hemisphere, and focused our analyses on the dorsal pallium, where progenitor cells are widely separated, facilitating the recovery of individual cell clones (Fig. 4A,B). We considered that two cells belong to one clone when they were in direct contact with each other. In slices with distinct cell groups, cell clones were

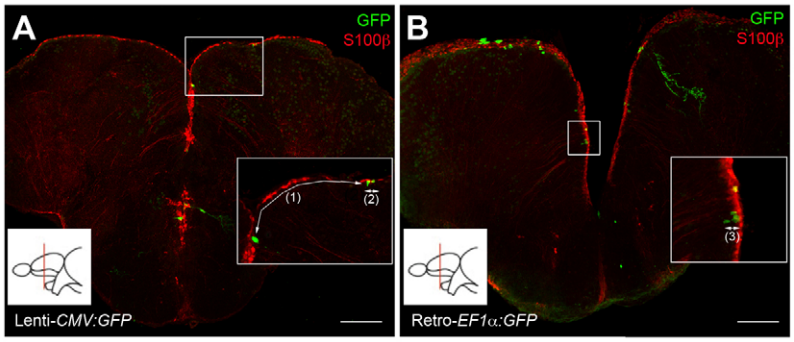

C

distance	min-max in µm (average)	estimated from n clones
(1) distance between two cell clones	26-260 (64)	n=29
(2) distance between two cells in a clone	4-17 (9)	n=21
(3) distance of neurons from the VZ	7-14 (9)	n=12
(4) distance of two glial cells from next glia	38-260 (95)	n=4

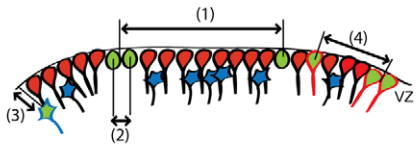

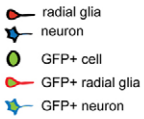

Fig. 4. Conditions used for clonal analyses. (**A**,**B**) Composite *z*-stack images of typical slices analyzed, showing the density of single cells and cell clones per slice, revealed in a double immunocytochemistry for GFP (green) and S100β (red). Insets show magnified views of the boxed areas, numbers in brackets refer to the distances described in C. Scale bars: 100 µm. (**C**) Distance separating clones and cells within a clone at 28 dpi. We considered as a single clone cells that were adjacent (distance between cell centers reached a maximum of 17 µm in one case with two very elongated cells), and separated from the next cell (group) by at least 25 µm. *n*, number of clones counted from a minimum of four sections from four brains for each distance.

separated by 25 µm or more (Fig. 4C). During the time frame of this analysis (3-4 weeks), adult-born neurons in the pallium exhibit extremely limited migration (Adolf et al., 2006), a finding that we confirmed by measuring the average distance of neuronal GFP cell clones from the VZ (average: 9 µm, Fig. 4C). The same was observed for adult-born radial glia (see Fig. 5A-C): doublets of GFP-positive glial cells always consisted in adjacent cells, in an environment where the next glial clone at the VZ was further than 38 µm apart (Fig. 4C).

Overall, 50 and 22 isolated cell clusters could be analyzed in brains transduced respectively with retro- and lentiviruses at 21-28 dpi (Fig. 5I,J). To assess cell identity, S100β, HuC/D and GFP expression were analyzed. Given that the near entirety of cells born during this time are either radial glia or neurons [Fig. 2, and Adolf et al. (Adolf et al., 2006)], we considered S100β-negative cells to be fated towards a neuronal identity in cases where only a double labeling for S100β and GFP was used. The size of the clones recovered during the time frame analyzed was of one or two cells. As retroviruses only transduce one of the daughter cells of the infected progenitor (Hajihosseini et al., 1993), single-cell clones are made of this daughter cell that has not undergone any further division. Two-cell clones are the progeny of this daughter, which divided during the 28 dpi. Because lentiviruses also transduce non-dividing cells, single-cell clones can be quiescent or differentiated cells that were directly transduced, while two-cell clones are the direct progeny of a transduced NPC.

Because the two viruses target type I and III progenitor cells in different proportions (Fig. 1), a global comparison of the clones obtained in both cases permits comparing the fate of these distinct progenitors at the population level. During the 4 weeks of the experiment, lentivirus-transduced cells appeared to produce mostly glial cells (90% of clones with a glial fate only, Fig. 5A,B,J) (significance compared with other clone types: P=0.0005, unpaired *t*-test) while retroviral transduction marked similar proportions of glial-only and neuronal-only clones (36% and 56% of cases, respectively) (Fig. 5C-E,I). Given the different tropism of the two viruses (Fig. 1), this result indicates that, within 4 weeks, type I progenitors are mostly quiescent or undergoing gliogenic divisions, while type III cells generate neurons. This is in agreement with the fact that type III cells express neuroblast markers such as *ascl1a* (Chapouton et al., 2010). The size of the 'neuron-only' clones obtained following retroviral infection further suggests that type III cells generally undergo one or two divisions (during the 4 weeks of the experiment), and that their final division is generally symmetric neurogenic, generating two neurons. Indeed, having observed little or no cell death at any time point within the radial glia layer of the VZ in parallel experiments (not shown, see also Fig. S2C in the supplementary material), we consider it unlikely that glial cells would be generated in such divisions and subsequently die. At least half of the type III progenitors transduced underwent a final division (64% of the 'neuron-only' clones comprise one single cell), further suggesting that the population of type III cells shows only a very limited amplification potential.

Finally, we used the lentivirus experiments to trace predominantly type I progenitors (see Fig. 1) and assess their self-renewal and potency to generate different cell types. The high proportion of single radial glial cells recovered (63%), of which a majority are progenitors (Chapouton et al., 2010), attests the very long cell cycle of type I cells (significance of one-cell compared with two-cell glial clones: P=0.02, unpaired *t*-test). In contrast to the situation observed using retroviruses, the majority of two-cell clones recovered following lentiviral transduction contained at least one glial cell (Fig. 5J), suggesting that type I/II progenitors seem not or very rarely to undergo a terminal symmetric neurogenic division (significance compared with retrovirus-traced one- and two-cell clones: P=0.01, Fisher's exact test). Eighty-six percent of the two-cell clones recovered were composed of two radial glia (significance compared with other two-cell lentiviral clone types: P<0.0001, unpaired *t*-test), demonstrating the predominant occurrence of slow symmetric gliogenic divisions within the

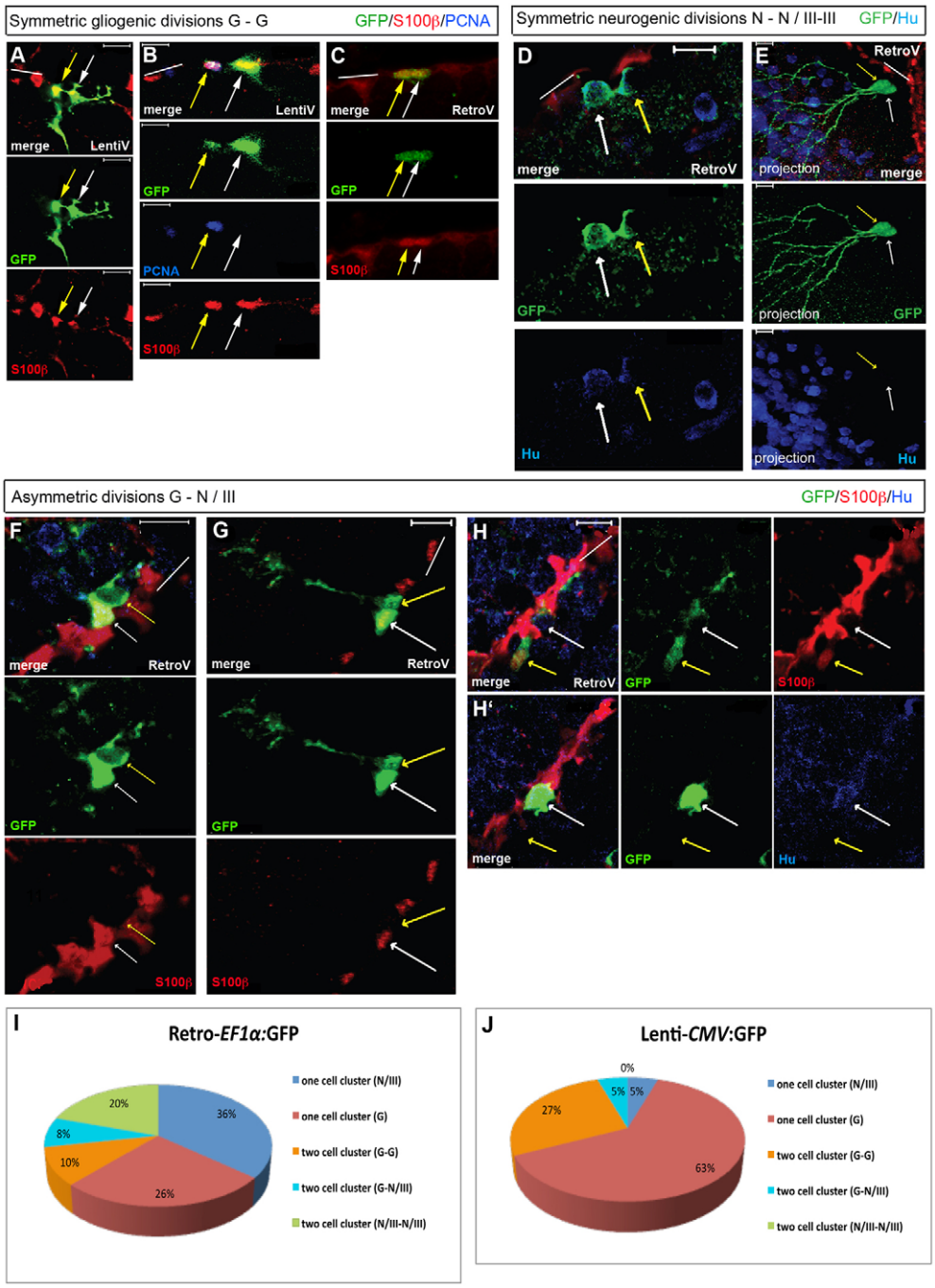

Fig. 5. Analysis of cell divisions at the single cell level. All brains were analyzed at 21-28 dpi. Brain sections were immunostained with GFP, S100β (red), HuC/D or PCNA. We considered S100β-negative cells to be fated towards a neuronal identity in cases where only a double labeling for S100β and GFP was used (cells referred to as 'III', indicating a neuroblast identity). S100β-positive cells are identified as glia ('G') and HuC/D-positive cells as neurons ('N') (single confocal planes of merged fluorescence and single fluorescence pictures, ventricular zone indicated by white bars). In E, a projection of several confocal stacks is illustrated; the two daughter cells are indicated by white and yellow arrows. (**A-C**) Gliogenic divisions ('G-G') observed after lentiviral (A,B) or retroviral (C) transduction. In B, the section is stained for PCNA, illustrating self-renewal. (**D**,**E**) Symmetric neurogenic divisions traced using a retrovirus. In both cases, the GFP-positive daughters are located away from the VZ (red). In E, these cells do not express detectable HuC/D levels, but harbor a developed dendritic tree. (**F-H'**) Asymmetric divisions generating a radial glia and a S100β-negative neuroblast (F,G) or neuron (H) (H and H' are two adjacent focal planes of the same section). (**I**,**J**) Quantification of the one- and two-cell clones observed after 21-28 dpi for each viral type (retrovirus: 50 cell clones in four brains, lentivirus: 22 cell clones in four brains). Scale bars: 10 μm.

population of radial glial stem cells. To assess whether the gliogenic divisions traced from type I/II cells could be self-renewing, we analyzed PCNA expression in two-cell clones, and could indeed recover cases where at least one S100β-positive glial daughter cell was again in division (Fig. 5B).

By focusing on mixed clones, we next addressed cell differentiation potential at the single cell level. We recovered 14% of mixed clones composed of one glia and one non-glial cell among two-cell clusters in lentiviral infections (5% of the total clone types recovered) (Fig. 5J), and a similar proportion (21%; 8% of the total clone types) in retroviral infections (Fig. 5F-I). In one case, the non-glial daughter could be identified as HuC/D positive (Fig. 5H), hence directly illustrating the generation of both neuronal and glial cells from a single progenitor/stem cell. Most non-glial daughters were negative for HuC/D, suggesting their neuroblast identity (Fig. 5F). These results demonstrate that the pallial VZ hosts NPCs that are at least bi-potent at the single cell level.

Notch signaling decreases the division rate of type I and III cells without major effect on their division mode

Notch pathway components are expressed at the zebrafish adult telencephalic VZ, and blocking Notch signaling increases the proportion of dividing NPCs in that location (Chapouton et al., 2010). Blocking Notch may increase proliferation within the radial glia population; however, given that type III cells divide faster than type I/II cells, it may also bias the division mode or the identity of

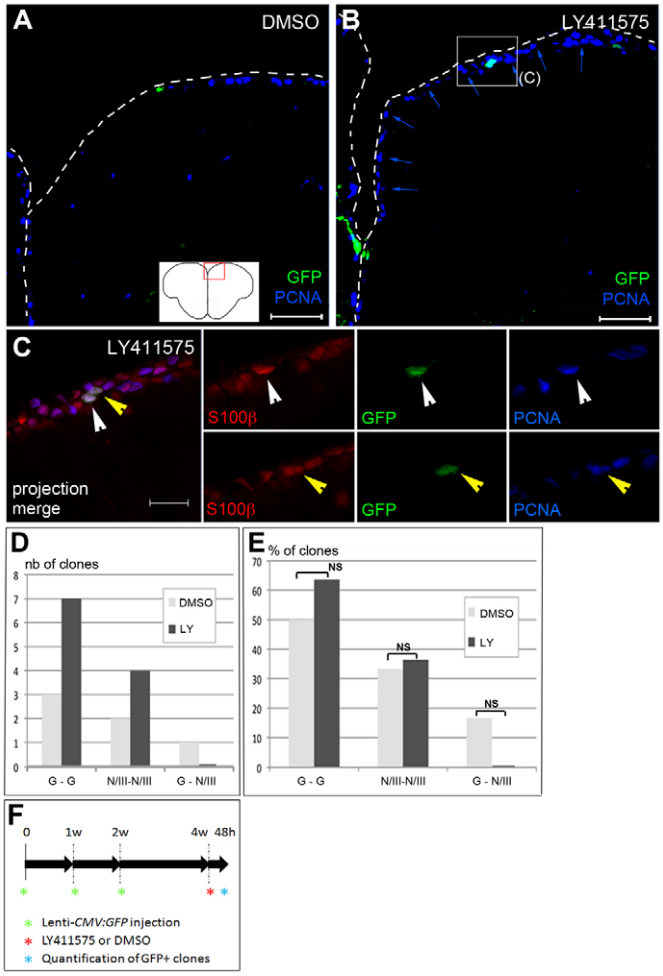

Fig. 6. Notch activity modulates proliferation rate within the glia and neuroblast populations. (**A**,**B**) Effect of Notch blockade on cell proliferation at the VZ 14-28 days after lentiviral injection (see F), visualized on cross-sections double-stained for GFP (green) and PCNA (blue) (ventricle delimited by the dotted line). Scale bars: 50 μm. (**C**) Example of a symmetric gliogenic division occurring upon Notch blockade. The section is triple-stained for S100β (red), GFP (green) and PCNA (blue). The left panel is the merged image of the boxed area in B (confocal projection of a 7 μm stack) and right panels are single channel views of optical sections taken at different *z* planes to visualize the two daughter cells (white and yellow arrowheads). Both cells are PCNA positive. Scale bar: 20 μm. (**D**,**E**) Number of clones (D) and proportion of clones (E) of each division type (G-G, symmetric gliogenic; III-III, symmetric neurogenic; G-N/III, asymmetric) in control (DMSO) or LY411575 (LY)-treated brains 14-28 days after lentiviral injection. In E, *P*>0.3 in a Fisher's exact test. Number of PCNA-positive glial cells generated from G-G divisions: two in DMSO-treated and four in LY-treated brains. (**F**) Scheme of the Notch blockade experiment.

radial glia towards the generation of type III cells, leading to a net increase in the number of VZ divisions. In addition, and non-exclusively, Notch may accelerate the divisions of type III cells, and/or their number of divisions. To address these issues, we followed the number, size and identity of lentiviral cell clones upon Notch blockade, by applying the γ-secretase inhibitor LY411575 (LY) to the fish swimming water for 48 hours at 14-28 dpi (Fig. 6F). As reported with the γ-secretase inhibitor DAPT (Chapouton et al., 2010), LY treatment led to a strong increase of VZ proliferation (Fig. 6A,B). In accordance with this, the number of two-cell lentiviral clones counted at the VZ was higher in LY-treated than in control fish (1.8 times increase, 80 sections from eight brains analyzed in each case; P=0.04, unpaired t-test). When analyzing two-cell clone identities, we further observed that the proportions of the different clone subtypes were unchanged between control and treated brains. First, a high number of clones composed of two glial cells (G-G) was counted (Fig. 6C,D), in similar proportions to controls (P=0.64, Fisher's exact test) (Fig. 6E), indicating that symmetric gliogenic divisions are not impaired by Notch blockade. The proportion of self-renewing G-G divisions, i.e. the number of PCNA-positive glial cells generated from these divisions, was identical in the two treatment conditions (29%, P=1, unpaired t-test) (not shown). For both treatments we observed very low frequencies of asymmetrical divisions (one case, 17% of cases in controls, no cases in LY-treated fish) (Fig. 6E). Finally, the number of symmetric neurogenic divisions (N/III-N/III) was also increased, and their proportion among other division types remained identical to controls (Fig. 6D,E) (P=1, Fisher's exact test). The size of neurogenic clones was also unchanged (two cells in each of the four clones recorded) (not shown). Together, the most parsimonious interpretation of these observations is that blocking Notch increases the amount of symmetric gliogenic divisions without exerting a major effect on the division mode of type I cells.

DISCUSSION

Clonal analyses using retroviral tracing

Our study demonstrates the efficacy of retro- and lentiviruses to label and trace a variety of cell types in the adult zebrafish brain. A major step forward of this technique is to permit clonal analysis. Several potential caveats, such as lumping, splitting and clumping errors, have been characterized for such approaches (Costa et al., 2009). Two cells in adjacent positions may be erroneously 'lumped' together into a single clone, although they are the progeny of two different progenitor cells (e.g. through cell migration or through the clumping of viral particles that will infect neighboring progenitors). Conversely, daughter cells may 'split' a clone by migrating apart from each other. The very limited migration of adult-born neurons and glia in the zebrafish adult pallium (Adolf et al., 2006) and our selection of slices with few cell clones strongly minimize such risks. However, real-time analyses would be required to fully rule them out. Clumping has been considered minimal in previous analyses in mouse (Cepko et al., 1998). Here, lentiviruses generated a large majority (68%) of single-cell clones, arguing against a high frequency of neighboring infections. All other clones had no more than two cells, which, if resulting from clumping, could only be explained by the targeting of two neighboring non-dividing cells, systematically excluding dividing NPCs. Our retro- and lentiviruses possess the same envelope, so they should clump to a similar degree. These observations strongly suggest that clumping only influences our results to a minor degree.

Lineage and amplification potential of telencephalic progenitor subtypes

Three progenitor subtypes have been classified at the zebrafish adult telencephalic VZ, of which types I and II are radial glia in, respectively, their quiescent and dividing phases; type III are dividing neuroblasts (Chapouton et al., 2010; März et al., 2010). The present clonal analysis now supports a lineage relationship between progenitor types I/II and III, given the recovery of

mixed two-celled clones composed of one radial glia and a ventricular non-glial cell (Fig. 5F,G), most likely a neuroblast. In addition, the different fates of retro- and lentivirus-transduced cells indicate that the majority of HuC/D-positive neurons generated within 4 weeks originate from state III progenitors. Indeed, 56% of retroviral clones, which originated mostly from type III cells (Fig. 1), were neuronal, against 10% for lentiviral tracing. Together, these results support the existence of an endogenous transition between progenitor types I/II and III during neuronal generation.

Variations have been observed in the mouse in the amplification potential of the 'dividing neuroblast' cell type depending on its location: 'transit-amplifying progenitors' (type C cells) undergo multiple divisions before neuronal differentiation along the SEZ and RMS (Doetsch et al., 1999; Doetsch et al., 2002), whereas type 3 cells at the SGZ only divide a few times (Hayes and Nowakowski, 2002; Seri et al., 2001; Steiner et al., 2006; Suh et al., 2007). We report here that the amplification potential of pallial type III progenitors is generally low, while in the subpallium we frequently observed the migration of HuC/D-positive newborn neurons along chain-like structures of up to 6-10 cells at 14 dpi (see Fig. 2A). Although the density of infected cells in this area precluded clonal analysis, the aligned organization of GFP-positive neurons suggests that they would originate from a single progenitor having undergone multiple divisions. Different rates of cell death may also contribute to the different neuronal clone sizes of these two regions.

Telencephalic VZ progenitors display self-renewal and the capacity to generate different cell types at the single cell level

Multipotency of the telencephalic germinal zone was previously observed at the population level using BrdU labeling (Adolf et al., 2006; Chapouton et al., 2007; Grandel et al., 2006; März et al., 2010; Pellegrini et al., 2007). Here, we analyze for the first time the progeny of single cells and could identify mixed clones consisting of S100β-positive and S100β-negative/HuC/D-positive cells, demonstrating the generation of asymmetrical fates from single VZ progenitors. Because lentiviruses exhibited a very strong preference for type I/II progenitors, we consider it most likely that these mixed cell clones originate from the latter progenitor type. We cannot formally rule out that the few type III cells also targeted by the lentivirus (Fig. 1) contribute to this phenotype. However, should type III cells undergo asymmetrical divisions, we would have expected a much higher proportion of asymmetrical fates in retrovirus transductions, given that retroviruses target a majority of type III cells (Fig. 1).

The other defining property of NSC is self-renewal. Using lentiviruses, with which 92% of transduced pallial VZ cells are radial glia (Fig. 1), we obtained here the first method to trace directly the quiescent type I cell population. The large majority of two-celled clones contained at least one radial glia, and we identified cases where one at least of the generated glial cells maintain the capacity to proliferate (Fig. 5B,I). These results demonstrate the self-renewing potential of radial glial cells in the zebrafish adult pallium. The low incidence of such cells, both in the zebrafish and mouse systems, may be only apparent, reflecting snap-shot analyses, or might reveal a subpopulation of radial glia endowed with self-renewal properties. Together, our analyses nevertheless support the existence of radial glia progenitor cells with single cell properties similar to those demonstrated for mammalian adult NSCs.

Prominent occurrence of symmetrical divisions within the adult radial glia population may underlie the maintenance of widespread germinal zones in the adult zebrafish brain

Symmetrical versus asymmetrical self-renewing divisions condition how differentiation can be ensured while preserving stem cell pools. Although asymmetrical self-renewing divisions allow the generation of committed precursors and maintain a constant number of SCs, symmetrical divisions expand SC pools. Overall, asymmetrical divisions seem predominant under steady-state conditions in self-renewing tissues, while symmetrical divisions characterize early development and regenerative processes (Chenn and McConnell, 1995; Morrison and Kimble, 2006; Noctor et al., 2004; Noctor et al., 2008) (reviewed by Farkas and Huttner, 2008; Gotz and Huttner, 2005). The situation in the adult brain remains incompletely understood, such analyses being hampered by the difficulty of direct imaging in vivo, and the rarity of divisions from quiescent progenitors. Asymmetrical NSC divisions were reported both in the SEZ (Morshead et al., 1998) and SGZ (Suh et al., 2007) through retroviral-mediated tracing, and may predominate in the adult mouse germinal zones. By contrast, the symmetrical division of adult NSCs is suggested from in vitro evidence in neurospheres, but may be rare in vivo (Suh et al., 2007). Our results suggest that the situation in the zebrafish adult pallium is strikingly different, with a majority of lentivirus-traced two-celled clones being composed of two radial glia (Fig. 5J). Because most radial glia are likely to be progenitors (Chapouton et al., 2010; März et al., 2010), symmetrical divisions within the radial glia population will tend to amplify the radial glia progenitor pool. We propose that this phenomenon may be very relevant to avoid NSC depletion and maintain widespread constitutive neurogenesis during post-embryonic life in the zebrafish brain. Among other possibilities, this may be linked to the fact that the adult zebrafish brain still grows hence needs to keep enhancing its progenitor/SC pool during adulthood. In this context, it will be important to identify the mechanisms controlling symmetrical versus asymmetrical divisions within the adult zebrafish radial glia population, and to assess the maintenance of this division mode under pathological and aging conditions.

Notch signaling primarily maintains the population of quiescent adult radial glia through controlling cell cycle speed

We have recently identified Notch as a major maintenance factor for quiescent radial glial cells at the zebrafish adult telencephalic VZ (Chapouton et al., 2010). These results are in agreement with recent invalidations of canonical Notch signaling in the adult mouse SEZ (Imayoshi et al., 2010) and SGZ (Ehm et al., 2010), suggesting a conserved role for Notch in controlling the proliferation characteristics of adult germinal zones. Long-term analyses, as well as neurosphere and reconstitution assays, further indicated that mouse adult germinal zones were progressively depleted in NSCs upon Notch invalidation (Ables et al., 2010; Ehm et al., 2010; Imayoshi et al., 2010). Together, these observations suggest that Notch maintains NSC self-renewal properties and limits the transition from NSCs to amplifying progenitors. This scenario may also account for the increased proliferation observed at the zebrafish telencephalic VZ upon Notch blockade (Chapouton et al., 2010), given the faster cycle of type III, as opposed to radial glial, cells: hence, if type I cells were to lose their NSC potential upon Notch blockade and transit to the type III state, a net increase in proliferation would follow. The single-cell analysis of division

modes presented in the present paper allows addressing this issue directly. Although we did not record late time points after LY treatment, our results highlight an outcome different from expected based on mouse data. Indeed, following Notch blockade: (1) symmetric gliogenic divisions are maintained and their number is increased; (2) the proportion of self-renewing divisions within this category is preserved; and (3) we failed to reveal any bias in the proportions of the different neural progenitor division types at the VZ (Fig. 6). Given the low incidence of asymmetrical divisions in type I cells (Fig. 5), it is very unlikely that the increased number of symmetric gliogenic divisions in this cell type results from a switch from the asymmetrical to the symmetrical mode. Together, our results therefore suggest that, in the context of the zebrafish adult pallium, Notch plays a new and prominent role in primarily controlling the proliferation rate of NSC, without a visible effect on NSC identity and fate. Whether Notch actually slows down the cell cycle of type I cells, or delays cell cycle re-entry, is an interesting issue that will require attention in the future. The divergent outcome of Notch blockade in zebrafish and mouse may reflect a true difference of the NSCs status between species. Alternatively, it may result from the overrepresentation of symmetrical NSC divisions in zebrafish, making them more easily observable. Along these lines, the status of asymmetrical divisions, largely under-represented in the present study, will need to be addressed with caution. The increased number of symmetric neurogenic divisions, without changing their proportion at the VZ nor affecting neuroblast expansion, may follow from the increased generation of NSCs or reflect a direct effect of Notch on type III progenitors.

Functional integration of adult-born neurons

We also used retroviral labeling to analyze for the first time the maturation and connectivity of single GFP-positive newborn neurons in the adult zebrafish telencephalon. We show that these neurons express the synaptic vesicle marker SV2, which labels presynaptic terminals, in the zebrafish subpallial and pallial circuitries. A similar situation was reported in the mouse 8 weeks after infection (Markakis and Gage, 1999; van Praag et al., 2002). Using electrophysiological recordings, we further demonstrate action potential firing in neurons starting around 7 weeks after birth. This structural and functional integration of new neurons is probably the first hint that, in the zebrafish (as in mouse), adult-born neurons might contribute to the variety of growth and plasticity events that ensure the control of brain physiology and behavior. The low incidence of neuronal death reported here during neuronal maturation further suggests that the remodeling of neuronal circuits during the adult life of the zebrafish may be massive.

Acknowledgements

We thank colleagues from the previous and current Bally-Cuif laboratory and the fish house teams at the HMGU and CNRS, and Isabelle Foucher, Alessandro Alunni and Kim Dale for help in setting up the LY411575 technique. The SV2 antibody was obtained from the Developmental Studies Hybridoma Bank developed under the auspices of the NICHD and maintained by the University of Iowa, Department of Biology, Iowa City, IA 52242. LY411575 was obtained as a gift from Chemical Synthesis Core Facility, Mayo Clinic Jacksonville, Jacksonville, FL 32224, USA. I.R. was supported by the Ecole des Neurosciences de Paris and a fellowship within the Post-Doctoral Program of the DAAD. Work in the L.B.C. laboratory at the HMGU was funded by the Helmholtz Association, the EU ZF-Models project (contract number LSHG-CT-2003-503466) and the Center for Protein Science-Munich (CIPSM). For work at the CNRS, funds from the EU projects NeuroXsys and ZF-Health, the ANR, the ENP, the FRM, the PIME program and the Schlumberger Association are greatly acknowledged. J.A.H. was supported by ANR-07-NEUR-007-1 to G.F.

Competing interests statement

The authors declare no competing financial interests.

Supplementary material

Supplementary material for this article is available at
http://dev.biologists.org/lookup/suppl/doi:10.1242/dev.058156/-/DC1

References

Ables, J. L., Decarolis, N. A., Johnson, M. A., Rivera, P. D., Gao, Z., Cooper, D. C., Radtke, F., Hsieh, J. and Eisch, A. J. (2010). Notch1 is required for maintenance of the reservoir of adult hippocampal stem cells. *J. Neurosci.* **30**, 10484-10492.

Adolf, B., Chapouton, P., Lam, C. S., Topp, S., Tannhauser, B., Strahle, U., Gotz, M. and Bally-Cuif, L. (2006). Conserved and acquired features of adult neurogenesis in the zebrafish telencephalon. *Dev. Biol.* **295**, 278-293.

Brill, M. S., Snapyan, M., Wohlfrom, H., Ninkovic, J., Jawerka, M., Mastick, G. S., Ashery-Padan, R., Saghatelyan, A., Berninger, B. and Gotz, M. (2008). A dlx2- and pax6-dependent transcriptional code for periglomerular neuron specification in the adult olfactory bulb. *J. Neurosci.* **28**, 6439-6452.

Burns, J. C., Friedmann, T., Driever, W., Burrascano, M. and Yee, J. K. (1993). Vesicular stomatitis virus G glycoprotein pseudotyped retroviral vectors: concentration to very high titer and efficient gene transfer into mammalian and nonmammalian cells. *Proc. Natl. Acad. Sci. USA* **90**, 8033-8037.

Carleton, A., Petreanu, L. T., Lansford, R., Alvarez-Buylla, A. and Lledo, P. M. (2003). Becoming a new neuron in the adult olfactory bulb. *Nat. Neurosci.* **6**, 507-518.

Cepko, C. L., Ryder, E., Austin, C., Golden, J., Fields-Berry, S. and Lin, J. (1998). Lineage analysis using retroviral vectors. *Methods* **14**, 393-406.

Chapouton, P., Jagasia, R. and Bally-Cuif, L. (2007). Adult neurogenesis in non-mammalian vertebrates. *BioEssays* **29**, 745-757.

Chapouton, P., Skupien, P., Hesl, B., Coolen, M., Moore, J. C., Madelaine, R., Kremmer, E., Faus-Kessler, T., Blader, P., Lawson, N. D. et al. (2010). Notch activity levels control the balance between quiescence and recruitment of adult neural stem cells. *J. Neurosci.* **30**, 7961-7974.

Chen, W., Burgess, S., Golling, G., Amsterdam, A. and Hopkins, N. (2002). High-throughput selection of retrovirus producer cell lines leads to markedly improved efficiency of germ line-transmissible insertions in zebra fish. *J. Virol.* **76**, 2192-2198.

Chenn, A. and McConnell, S. K. (1995). Cleavage orientation and the asymmetric inheritance of Notch1 immunoreactivity in mammalian neurogenesis. *Cell* **82**, 631-641.

Colak, D., Mori, T., Brill, M. S., Pfeifer, A., Falk, S., Deng, C., Monteiro, R., Mummery, C., Sommer, L. and Gotz, M. (2008). Adult neurogenesis requires Smad4-mediated bone morphogenic protein signaling in stem cells. *J. Neurosci.* **28**, 434-446.

Costa, M. R., Bucholz, O., Schroeder, T. and Gotz, M. (2009). Late origin of glia-restricted progenitors in the developing mouse cerebral cortex. *Cereb. Cortex* **19 Suppl. 1**, i135-i143.

Deng, W., Aimone, J. B. and Gage, F. H. (2010). New neurons and new memories: how does adult hippocampal neurogenesis affect learning and memory? *Nat. Rev. Neurosci.* **11**, 339-350.

Doetsch, F., Garcia-Verdugo, J. M. and Alvarez-Buylla, A. (1999). Regeneration of a germinal layer in the adult mammalian brain. *Proc. Natl. Acad. Sci. USA* **96**, 11619-11624.

Doetsch, F., Petreanu, L., Caille, I., Garcia-Verdugo, J. M. and Alvarez-Buylla, A. (2002). EGF converts transit-amplifying neurogenic precursors in the adult brain into multipotent stem cells. *Neuron* **36**, 1021-1034.

Ehm, O., Goritz, C., Covic, M., Schaffner, I., Schwarz, T. J., Karaca, E., Kempkes, B., Kremmer, E., Pfrieger, F. W., Espinosa, L. et al. (2010). RBPJkappa-dependent signaling is essential for long-term maintenance of neural stem cells in the adult hippocampus. *J. Neurosci.* **30**, 13794-13807.

Farkas, L. M. and Huttner, W. B. (2008). The cell biology of neural stem and progenitor cells and its significance for their proliferation versus differentiation during mammalian brain development. *Curr. Opin. Cell Biol.* **20**, 707-715.

Fauq, A. H., Simpson, K., Maharvi, G. M., Golde, T. and Das, P. (2007). A multigram chemical synthesis of the gamma-secretase inhibitor LY411575 and its diastereoisomers. *Bioorg. Med. Chem. Lett.* **17**, 6392-6395.

Ganz, J., Kaslin, J., Hochmann, S., Freudenreich, D. and Brand, M. (2010). Heterogeneity and Fgf dependence of adult neural progenitors in the zebrafish telencephalon. *Glia* **58**, 1345-1363.

Ge, S., Goh, E. L., Sailor, K. A., Kitabatake, Y., Ming, G. L. and Song, H. (2006). GABA regulates synaptic integration of newly generated neurons in the adult brain. *Nature* **439**, 589-593.

Gotz, M. and Huttner, W. B. (2005). The cell biology of neurogenesis. *Nat. Rev. Mol. Cell Biol.* **6**, 777-788.

Grandel, H., Kaslin, J., Ganz, J., Wenzel, I. and Brand, M. (2006). Neural stem cells and neurogenesis in the adult zebrafish brain: origin, proliferation dynamics, migration and cell fate. *Dev. Biol.* **295**, 263-277.

Hajihosseini, M., Iavachev, L. and Price, J. (1993). Evidence that retroviruses integrate into post-replication host DNA. *EMBO J.* **12**, 4969-4974.
Hayes, N. L. and Nowakowski, R. S. (2002). Dynamics of cell proliferation in the adult dentate gyrus of two inbred strains of mice. *Brain Res. Dev. Brain Res.* **134**, 77-85.
He, S., Salas-Vidal, E., Rueb, S., Krens, S. F., Meijer, A. H., Snaar-Jagalska, B. E. and Spaink, H. P. (2006). Genetic and transcriptome characterization of model zebrafish cell lines. *Zebrafish* **3**, 441-453.
Imayoshi, I., Sakamoto, M., Yamaguchi, M., Mori, K. and Kageyama, R. (2010). Essential roles of Notch signaling in maintenance of neural stem cells in developing and adult brains. *J. Neurosci.* **30**, 3489-3498.
Jackson-Lewis, V., Vila, M., Djaldetti, R., Guegan, C., Liberatore, G., Liu, J., O'Malley, K. L., Burke, R. E. and Przedborski, S. (2000). Developmental cell death in dopaminergic neurons of the substantia nigra of mice. *J. Comp. Neurol.* **424**, 476-488.
Jeon, B. S., Kholodilov, N. G., Oo, T. F., Kim, S. Y., Tomaselli, K. J., Srinivasan, A., Stefanis, L. and Burke, R. E. (1999). Activation of caspase-3 in developmental models of programmed cell death in neurons of the substantia nigra. *J. Neurochem.* **73**, 322-333.
Jontes, J. D., Emond, M. R. and Smith, S. J. (2004). In vivo trafficking and targeting of N-cadherin to nascent presynaptic terminals. *J. Neurosci.* **24**, 9027-9034.
Kriegstein, A. and Alvarez-Buylla, A. (2009). The glial nature of embryonic and adult neural stem cells. *Annu. Rev. Neurosci.* **32**, 149-184.
Lin, S., Gaiano, N., Culp, P., Burns, J. C., Friedmann, T., Yee, J. K. and Hopkins, N. (1994). Integration and germ-line transmission of a pseudotyped retroviral vector in zebrafish. *Science* **265**, 666-669.
Lledo, P. M. and Saghatelyan, A. (2005). Integrating new neurons into the adult olfactory bulb: joining the network, life-death decisions, and the effects of sensory experience. *Trends Neurosci.* **28**, 248-254.
Lledo, P. M., Alonso, M. and Grubb, M. S. (2006). Adult neurogenesis and functional plasticity in neuronal circuits. *Nat. Rev. Neurosci.* **7**, 179-193.
Markakis, E. A. and Gage, F. H. (1999). Adult-generated neurons in the dentate gyrus send axonal projections to field CA3 and are surrounded by synaptic vesicles. *J. Comp. Neurol.* **406**, 449-460.
Marz, M., Chapouton, P., Diotel, N., Vaillant, C., Hesl, B., Takamiya, M., Lam, C. S., Kah, O., Bally-Cuif, L. and Strahle, U. (2010). Heterogeneity in progenitor cell subtypes in the ventricular zone of the zebrafish adult telencephalon. *Glia* **58**, 870-888.
Morrison, S. J. and Kimble, J. (2006). Asymmetric and symmetric stem-cell divisions in development and cancer. *Nature* **441**, 1068-1074.
Morshead, C. M., Craig, C. G. and van der Kooy, D. (1998). In vivo clonal analyses reveal the properties of endogenous neural stem cell proliferation in the adult mammalian forebrain. *Development* **125**, 2251-2261.
Muller, F., Albert, S., Blader, P., Fischer, N., Hallonet, M. and Strahle, U. (2000). Direct action of the nodal-related signal cyclops in induction of sonic hedgehog in the ventral midline of the CNS. *Development* **127**, 3889-3897.
Niell, C. M., Meyer, M. P. and Smith, S. J. (2004). In vivo imaging of synapse formation on a growing dendritic arbor. *Nat. Neurosci.* **7**, 254-260.
Nissant, A., Bardy, C., Katagiri, H., Murray, K. and Lledo, P. M. (2009). Adult neurogenesis promotes synaptic plasticity in the olfactory bulb. *Nat. Neurosci.* **12**, 728-730.
Noctor, S. C., Martinez-Cerdeno, V., Ivic, L. and Kriegstein, A. R. (2004). Cortical neurons arise in symmetric and asymmetric division zones and migrate through specific phases. *Nat. Neurosci.* **7**, 136-144.
Noctor, S. C., Martinez-Cerdeno, V. and Kriegstein, A. R. (2008). Distinct behaviors of neural stem and progenitor cells underlie cortical neurogenesis. *J. Comp. Neurol.* **508**, 28-44.
Ory, D. S., Neugeboren, B. A. and Mulligan, R. C. (1996). A stable human-derived packaging cell line for production of high titer retrovirus/vesicular stomatitis virus G pseudotypes. *Proc. Natl. Acad. Sci. USA* **93**, 11400-11406.
Pellegrini, E., Mouriec, K., Anglade, I., Menuet, A., Le Page, Y., Gueguen, M. M., Marmignon, M. H., Brion, F., Pakdel, F. and Kah, O. (2007). Identification of aromatase-positive radial glial cells as progenitor cells in the ventricular layer of the forebrain in zebrafish. *J. Comp. Neurol.* **501**, 150-167.
Petreanu, L. and Alvarez-Buylla, A. (2002). Maturation and death of adult-born olfactory bulb granule neurons: role of olfaction. *J. Neurosci.* **22**, 6106-6113.
Pfeifer, A., Brandon, E. P., Kootstra, N., Gage, F. H. and Verma, I. M. (2001). Delivery of the Cre recombinase by a self-deleting lentiviral vector: efficient gene targeting in vivo. *Proc. Natl. Acad. Sci. USA* **98**, 11450-11455.
Pieper, A. A., Xie, S., Capota, E., Estill, S. J., Zhong, J., Long, J. M., Becker, G. L., Huntington, P., Goldman, S. E., Shen, C. H. et al. (2010). Discovery of a proneurogenic, neuroprotective chemical. *Cell* **142**, 39-51.
Seri, B., Garcia-Verdugo, J. M., McEwen, B. S. and Alvarez-Buylla, A. (2001). Astrocytes give rise to new neurons in the adult mammalian hippocampus. *J. Neurosci.* **21**, 7153-7160.
Steiner, B., Klempin, F., Wang, L., Kott, M., Kettenmann, H. and Kempermann, G. (2006). Type-2 cells as link between glial and neuronal lineage in adult hippocampal neurogenesis. *Glia* **54**, 805-814.
Suh, H., Consiglio, A., Ray, J., Sawai, T., D'Amour, K. A. and Gage, F. H. (2007). In vivo fate analysis reveals the multipotent and self-renewal capacities of Sox2+ neural stem cells in the adult hippocampus. *Cell Stem Cell* **1**, 515-528.
Toni, N., Teng, E. M., Bushong, E. A., Aimone, J. B., Zhao, C., Consiglio, A., van Praag, H., Martone, M. E., Ellisman, M. H. and Gage, F. H. (2007). Synapse formation on neurons born in the adult hippocampus. *Nat. Neurosci.* **10**, 727-734.
Toni, N., Laplagne, D. A., Zhao, C., Lombardi, G., Ribak, C. E., Gage, F. H. and Schinder, A. F. (2008). Neurons born in the adult dentate gyrus form functional synapses with target cells. *Nat. Neurosci.* **11**, 901-907.
van Praag, H., Schinder, A. F., Christie, B. R., Toni, N., Palmer, T. D. and Gage, F. H. (2002). Functional neurogenesis in the adult hippocampus. *Nature* **415**, 1030-1034.
Winner, B., Cooper-Kuhn, C. M., Aigner, R., Winkler, J. and Kuhn, H. G. (2002). Long-term survival and cell death of newly generated neurons in the adult rat olfactory bulb. *Eur. J. Neurosci.* **16**, 1681-1689.
Zhao, C., Teng, E. M., Summers, R. G., Jr, Ming, G. L. and Gage, F. H. (2006). Distinct morphological stages of dentate granule neuron maturation in the adult mouse hippocampus. *J. Neurosci.* **26**, 3-11.
Zhao, C., Deng, W. and Gage, F. H. (2008). Mechanisms and functional implications of adult neurogenesis. *Cell* **132**, 645-660.
Zupanc, G. K., Hinsch, K. and Gage, F. H. (2005). Proliferation, migration, neuronal differentiation, and long-term survival of new cells in the adult zebrafish brain. *J. Comp. Neurol.* **488**, 290-319.